Appl. Math. Mech. -Engl. Ed., **40**(1), 13–24 (2019)

Applied Mathematics and Mechanics (English Edition)

https://doi.org/10.1007/s10483-019-2407-8

Controlling a neuron by stimulating a coupled neuron*

Song LIANG[1], Zaihua WANG[1,2,†]

1. State Key Laboratory of Mechanics and Control of Mechanical Structures, Nanjing University of Aeronautics and Astronautics, Nanjing 210016, China;

2. Department of Basic Courses, Army Engineering University, Nanjing 211101, China

(Received Jul. 11, 2018 / Revised Sept. 10, 2018)

Abstract Despite the intensive studies on neurons, the control mechanism in real interactions of neurons is still unclear. This paper presents an understanding of this kind of control mechanism, controlling a neuron by stimulating another coupled neuron, with the uncertainties taken into consideration for both neurons. Two observers and a differentiator, which comprise the first-order low-pass filters, are first designed for estimating the uncertainties. Then, with the estimated values combined, a robust nonlinear controller with a saturation function is presented to track the desired membrane potential. Finally, two typical bursters of neurons with the desired membrane potentials are proposed in the simulation, and the numerical results show that they are tracked very well by the proposed controller.

Key words coupled neuron, observer-based control, spiking, bursting, robustness

Chinese Library Classification O29, O317$^+$.2

2010 Mathematics Subject Classification 34H05, 93C10

1 Introduction

Neurons are elementary units of the nervous system and have the ability to conduct signals rapidly over large distances. They receive, process, and transmit information by generating characteristic electrical pulses called action potentials or voltage spikes that occur when the membrane potential rapidly rises and falls. With the presence of external sensory stimuli, including light, sound, taste, smell, and touch, neurons change their activities by firing sequences of spikes in various temporal patterns. Although spikes can vary in duration, amplitude, and shape, they are typically treated as identical stereotyped events in neural coding studies. A number of mathematical models have been proposed for describing the phenomena of spikes, such as the Hodgkin-Huxley (HH) model[1], Morris-Lecar (ML) model[2], FitzHugh-Nagumo (FHN) model[3].

* Citation: LIANG, S. and WANG, Z. H. Controlling a neuron by stimulating a coupled neuron. *Applied Mathematics and Mechanics* (*English Edition*), **40**(1), 13–24 (2019) https://doi.org/10.1007/s10483-019-2407-8

† Corresponding author, E-mail: zhwang@nuaa.edu.cn

Project supported by the National Natural Science Foundation of China (No. 11372354) and the Jiangsu Innovation Program for Graduate Education (No. KYLX16_0308)

©The Author(s) 2019

The processes that generate only a single spike correspond to the depolarization, repolarization, and refractory period of the neuron. These processes are relatively simple. Repetitive spiking usually leads to more complicated dynamics, especially the bursting phenomenon. Bursting (burst firing) in a neuron is the potential, or chemical concentration changes between repetitive spiking and a quiescence state[4–5], and it has been found in many types of neurons, such as thalamic neurons[6] and dopamine-containing neurons of the mammalian midbrain[7]. Bursting patterns named Types I, II, $\cdots$, V have been introduced after Rinzel's work on the classification of bursting[4,8–10]. In view of a geometric bifurcation theory, Izhikevich[5] presented a complete classification, and suggested that the patterns of bursters should be named on the basis of the names of the two bifurcations involved instead of descriptions or the type plus the number, such as square-wave (Type I) burster, parabolic (Type II) burster, and elliptic (Type III) burster.

Apart from intrinsic properties of neurons, oscillatory activities may result from neural network properties, such as coupling strength and time delay[11]. Synchronization of coupled neurons is a phenomenon that has been studied extensively in Refs. [12]–[14]. Synchronization can be obtained for weakly connected networks[12], but not all weakly connected neurons can be synchronized[5,15–16]. While the coupling of neurons can be considered as a passive control strategy that has been a research topic of great interest over the past few decades, external stimuli can be regarded as active control strategies and have been used in some applications. Taking voluntary movement of the human body as an example, one can control some neurons to make coupled neurons do something specific, where the motor information is calculated in cortical areas and carried by upper motor neurons along the spinal cord to activate the lower motor neurons, and in turn to make the muscles contract. Motor cortex neurons were used to record signals for real-time device control in rats[17] and monkeys[18]. The study of the control (stimulus) mechanism among neurons has the potential to provide more accurate and effective stimuli in therapies by electrical nerve stimulation, such as transcutaneous electrical nerve stimulation (TENS) and neuromuscular electrical stimulation (NMES). Neuropeptide release by the electrical stimulation with different frequencies was introduced in Ref. [19]. In addition, a washout filter-aided dynamic feedback control was introduced to the Hindmarsh-Rose model neuron to change its type from Type II to Type I[20]. In Ref. [21], a feedback control was proposed for synchronization of two coupled FHN models. In Ref. [22], a kind of neural network was synchronized by using a single controller.

Some biological phenomena of neurons can be explained from the viewpoint of firing activity and synchronization, but the control mechanism of neurons has not been fully understood yet. It is still unclear what controllers are actually used in real interactions of neurons, and how to control their activities precisely. In the control design of coupled neurons, uncertainties should be taken into account, because it is hard to have the model parameters precisely measured, and the coupled neural systems are usually subject to the external disturbance. Thus, it is more reasonable to design the controller on the basis of measured signals. In this study, the track control of an uncertain neuron by stimulating another coupled uncertain neuron is studied. The following considerations distinguish this study from the previous works. (i) Uncertainties in neurons are taken into account, and only a controller can be used to make another neuron track a specified signal. (ii) Compared with the pinning control in neural networks, the strength of coupling has no particular limit, provided that it is not equal to 0. (iii) A robust controller with saturation function is presented in this paper.

2 Statement of the problem

The simplest control process between two neurons, as shown in Fig. 1, is considered. An appropriate stimulus on the neuron 1 is designed to make the coupled neuron 2 generate a desired action potential. The problem is a kind of track control of a two-dimensional system

with one controller, which can be mathematically described as

$$\begin{cases} \dot{u}_1 = f_1(u_1, \boldsymbol{w}_1) + k(u_1 - u_2) + d_1 + I(t), \\ \dot{\boldsymbol{w}}_1 = \boldsymbol{g}_1(u_1, \boldsymbol{w}_1), \\ \dot{u}_2 = f_2(u_2, \boldsymbol{w}_2) + k(u_2 - u_1) + d_2, \\ \dot{\boldsymbol{w}}_2 = \boldsymbol{g}_2(u_2, \boldsymbol{w}_2), \end{cases} \tag{1}$$

where u_1 and u_2 denote the membrane potentials of the neuron 1 and the neuron 2, respectively. In the HH model[1], $\boldsymbol{w}_1, \boldsymbol{w}_2 \in \mathbb{R}^3$ denote the three types of ion channels, i.e., a sodium channel with the index Na, a potassium channel with the index K, and an unspecific leakage channel with the resistance R. In the ML model[2], $\boldsymbol{w}_1, \boldsymbol{w}_2 \in \mathbb{R}^2$ (or $\mathbb{R}^1$) denote the Ca and K ion channels (or the K ion channel). In the FHN model[3], $\boldsymbol{w}_1, \boldsymbol{w}_2 \in \mathbb{R}^1$ denote recovery variables. The system (1) is also a generalized model of some other neuron models, such as the calcium-induced calcium release (CICR) model[23]. In mathematics, the functions f_1, f_2, $\boldsymbol{g}_1$, and $\boldsymbol{g}_2$ should be continuous and smooth with respect to $u_1, \boldsymbol{w}_1$ or $u_2, \boldsymbol{w}_2$. k denotes the coupling intensity, and $d_i = d_i(u_i, \boldsymbol{w}_i, t)$ $(i = 1, 2)$ denote the unknown stimuli from the external environment or other adjacent neurons or modeling error.

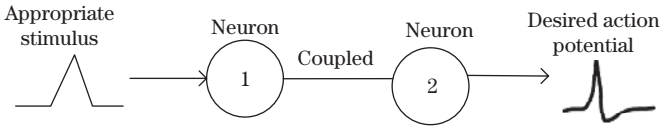

Fig. 1 Sketch map of the purpose of this paper

Assumption 1 The unknown terms d_i vary slowly, that is, there exist small positive numbers $\xi_i > 0$ such that $|\dot{d}_i| \leqslant \xi_i$ $(i = 1, 2)$.

The goal is to design an appropriate stimulus $I(t)$ to make u_2 track a desired membrane potential $u_{\mathrm{d}}(t)$ asymptotically and rapidly, that is, $u_2 - u_{\mathrm{d}}(t) \to 0$ as $t \to +\infty$ asymptotically and rapidly. Owing to the existence of uncertainties, it may be impossible to achieve such a goal. Therefore, a more realistic goal is to make $u_2 - u_{\mathrm{d}}(t) \to 0$ $(t \to +\infty)$ asymptotically, as far as possible.

3 Design of the stimulus $I(t)$

3.1 Observers and the differentiator

For the slowly varied uncertainty d_1, the observer is designed as

$$\begin{cases} \widehat{d_1} = y_1 + k_1 u_1, \\ \dot{y}_1 = -k_1 y_1 - k_1^2 u_1 - k_1(f_1(u_1, \boldsymbol{w}_1) + k(u_1 - u_2) + I(t)), \end{cases} \tag{2}$$

and for the slowly varied uncertainty d_2, the observer can be presented as

$$\begin{cases} \widehat{d_2} = y_2 + k_2 u_2, \\ \dot{y}_2 = -k_2 y_2 - k_2^2 u_2 - k_2(f_2(u_2, \boldsymbol{w}_2) + k(u_2 - u_1)), \end{cases} \tag{3}$$

where $\widehat{d_1}$ and $\widehat{d_2}$ are the observed values of d_1 and d_2, respectively, and the parameters k_1, $k_2 > 0$ are to be designed.

The principles of designing the observers (2) and (3) are similar to those found in other papers[24–25]. In most of these papers, the boundaries of $|d_i - \widehat{d}_i|$ for $i = 1, 2$ were calculated by means of the Lyapunov function. In the present study, the boundaries are estimated using the general solution formulae of ordinary differential equations with constant coefficients.

Theorem 1 *Under Assumption* 1, *consider the observers* (2) *and* (3) *for the system* (1). $\forall \epsilon > 0$, *there exist two sufficiently large numbers* $T_i > 0$ $(i = 1, 2)$ *such that*

$$|\widehat{d}_i - d_i| < \epsilon + k_i^{-1}\xi_i, \tag{4}$$

whenever $t > T_i$ $(i = 1, 2)$.

Proof Differentiating $\widehat{d}_1$ and $\widehat{d}_2$ in observers (2) and (3) with respect to time t and substituting the system (1) into them by $\dot{u}_1$ and $\dot{u}_2$, respectively, give

$$\dot{\widehat{d}}_i = -k_i\widehat{d}_i + k_i d_i \tag{5}$$

for $i = 1, 2$. It follows that

$$\dot{\widehat{d}}_i - \dot{d}_i = -k_i(\widehat{d}_i - d_i) - \dot{d}_i.$$

By using the general solution formulae for ordinary differential equations with constant coefficients, we get

$$\widehat{d}_i - d_i = \mathrm{e}^{-k_i(t-t_0)}(\widehat{d}_i(t_0) - d_i(t_0)) - \int_{t_0}^{t} \mathrm{e}^{-k_i(t-\tau)}\dot{d}_i(\tau)\mathrm{d}\tau,$$

and it goes to

$$\begin{aligned} |\widehat{d}_i - d_i| &= \mathrm{e}^{-k_i(t-t_0)}|(\widehat{d}_i(t_0) - d_i(t_0))| + \int_{t_0}^{t} \mathrm{e}^{-k_i(t-\tau)}|\dot{d}_i(\tau)|\mathrm{d}\tau \\ &\leqslant \mathrm{e}^{-k_i(t-t_0)}|(\widehat{d}_i(t_0) - d_i(t_0))| + k_i^{-1}\xi_i. \end{aligned} \tag{6}$$

Note that

$$\lim_{t\to+\infty} \mathrm{e}^{-k_i(t-t_0)}|(\widehat{d}_i(t_0) - d_i(t_0))| = 0.$$

Thus, $\forall \epsilon > 0$, there exist two sufficiently large numbers $T_i > 0$ $(i = 1, 2)$ such that Eq. (4) holds. This completes the proof.

According to Eq. (5), the designs of the observers (2) and (3) are similar to those of the first-order low-pass filters. The boundaries in Theorem 1 are also the maximum errors of the first-order low-pass filters.

Moreover, from Eq. (5), one has

$$\ddot{\widehat{d}}_i = -k_i\dot{\widehat{d}}_i + k_i\dot{d}_i.$$

Then, it follows that

$$\begin{aligned} |\dot{\widehat{d}}_i| &\leqslant \mathrm{e}^{-k_i(t-t_0)}|\dot{\widehat{d}}_i(t_0)| + k_i\int_{t_0}^{t} \mathrm{e}^{-k_i(t-\tau)}|\dot{d}_i(\tau)|\mathrm{d}\tau \\ &\leqslant \mathrm{e}^{-k_i(t-t_0)}|\dot{\widehat{d}}_i(t_0)| + (1 - \mathrm{e}^{-k_i(t-t_0)})\xi_i. \end{aligned}$$

Thus, one has

$$|\ddot{\widehat{d}}_i| \leqslant k_i\mathrm{e}^{-k_i(t-t_0)}|\dot{\widehat{d}}_i(t_0)| + (2k_i - k_i\mathrm{e}^{-k_i(t-t_0)})\xi_i. \tag{7}$$

Hence, $\ddot{\widehat{d}}_i$ is bounded for the system (1) and observers (2) and (3) under Assumption 1. Similarly, one can prove that the jth derivative $\widehat{d}_i^{(j)}$ is also bounded for $j = 1, 2, \cdots, n$. In the following, the estimated value of $\dot{\widehat{d}}_2$, denoted by v_2, is introduced by a traditional differentiator,

$$v_2(s) = \frac{s}{\gamma s + 1}\widehat{d}_2(s), \tag{8}$$

where γ is a small positive number. The state equation corresponding to the transfer function (8) is

$$\begin{cases} v_2(t) = \dfrac{1}{\gamma}(p(t) + \widehat{d}_2(t)), \\ \dot{p}(t) = -\dfrac{1}{\gamma}p(t) - \dfrac{1}{\gamma}\widehat{d}_2(t), \end{cases} \tag{9}$$

where $p(t)$ is an intermediate variable. The estimated error $v_2 - \dot{\widehat{d}}_2$ is given by the theorem below.

Theorem 2 *With the differentiator* (8) *or* (9)*, the estimated error of* $\dot{\widehat{d}}_2$ *has the following estimation.* $\forall \epsilon > 0$*, there exists a sufficiently large* $T_3 > 0$ *such that*

$$|v_2 - \dot{\widehat{d}}_2| < \epsilon + 2\gamma k_2 \xi_2,$$

whenever $t > T_3$*.*

Proof From Eq. (8) or Eq. (9), one has

$$\gamma \dot{v}_2 = -v_2 + \dot{\widehat{d}}_2(t), \tag{10}$$

which is equivalent to

$$\dot{v}_2 - \ddot{\widehat{d}}_2 = -\frac{1}{\gamma}(v_2 - \dot{\widehat{d}}_2(t)) - \ddot{\widehat{d}}_2.$$

Again, by using the general solution formulae of ordinary differential equations with constant coefficients, and taking the absolute value on both sides, one has

$$|v_2 - \dot{\widehat{d}}_2| \leqslant \mathrm{e}^{-\frac{1}{\gamma}(t-t_0)}|v_2(t_0) - \dot{\widehat{d}}_2(t_0)| + \int_{t_0}^{t} \mathrm{e}^{-\frac{1}{\gamma}(t-\tau)}|\ddot{\widehat{d}}_2(\tau)|\mathrm{d}\tau.$$

Note that

$$\int_{t_0}^{t} \mathrm{e}^{-\frac{1}{\gamma}(t-\tau)}\mathrm{e}^{-k_2(\tau-t_0)}\mathrm{d}\tau = \Big(\frac{1}{\gamma} - k_2\Big)^{-1}(\mathrm{e}^{-k_2(t-t_0)} - \mathrm{e}^{-\frac{1}{\gamma}(t-t_0)}) \tag{11}$$

together with Eq. (7), and one obtains

$$\begin{aligned} |v_2 - \dot{\widehat{d}}_2| \leqslant\ & \mathrm{e}^{-\frac{1}{\gamma}(t-t_0)}|v_2(t_0) - \dot{\widehat{d}}_2(t_0)| + k_2\Big(\frac{1}{\gamma} - k_2\Big)^{-1}(\mathrm{e}^{-k_2(t-t_0)} - \mathrm{e}^{-\frac{1}{\gamma}(t-t_0)})|\dot{\widehat{d}}_2(t_0)| \\ & + 2\gamma k_2 \xi_2. \end{aligned} \tag{12}$$

This theorem holds true, because $\mathrm{e}^{-\frac{1}{\gamma}(t-t_0)}|v_2(t_0) - \dot{\widehat{d}}_2(t_0)| + k_2(\frac{1}{\gamma} - k_2)^{-1}(\mathrm{e}^{-k_2(t-t_0)} - \mathrm{e}^{-\frac{1}{\gamma}(t-t_0)})$ $\cdot\, |\dot{\widehat{d}}_2(t_0)| \to 0$ as $t \to +\infty$.

3.2 Robust nonlinear control

Let $u_{\rm d}$ be the known and desired membrane potential for u_2 to track. Then, from the system (1), the error variable $u_2-u_{\rm d}$ satisfies

$$\begin{cases}\dot{u}_2-\dot{u}_{\rm d}=f_2(u_2,\boldsymbol{w}_2)+k(u_2-u_1)+d_2-\dot{u}_{\rm d},\\ \dot{u}_1=f_1(u_1,\boldsymbol{w}_1)+k(u_1-u_2)+d_1+I(t).\end{cases}\tag{13}$$

The main idea in the control design is to decompose the right hand side of the first equation of the system (13) into two parts, i.e., the stable term and the rest term. It is required to design an appropriate controller to make the rest term tend to 0 as far as possible, by using the second equation of the system (13). The details are given below.

The first equation of the system (13) can be rewritten as

$$\dot{u}_2-\dot{u}_{\rm d}=-a_1(u_2-u_{\rm d})+a_1(u_2-u_{\rm d})+f_2(u_2,\boldsymbol{w}_2)+k(u_2-u_1)+d_2-\dot{u}_{\rm d},$$

where $a_1>0$ is a number to be determined. Let $z=k^{-1}(a_1(u_2-u_{\rm d})+f_2(u_2,\boldsymbol{w}_2)+ku_2+d_2-\dot{u}_{\rm d})=k^{-1}((a_1+k)u_2+f_2(u_2,\boldsymbol{w}_2)+d_2-a_1u_{\rm d}-\dot{u}_{\rm d})$. Then, one has

$$\dot{u}_2-\dot{u}_{\rm d}=-a_1(u_2-u_{\rm d})+k(z-u_1).$$

Due to the existence of the unknown term d_2 in z, only the observed value of $\widehat{d_2}$ is available in the control design. Thus, one has

$$\dot{u}_2-\dot{u}_{\rm d}=-a_1(u_2-u_{\rm d})+k(\bar{z}-u_1)+d_2-\widehat{d}_2,$$

where $\bar{z}=k^{-1}((a_1+k)u_2+f_2(u_2,\boldsymbol{w}_2)+\widehat{d}_2-a_1u_{\rm d}-\dot{u}_{\rm d})$. Combining the second equation of the system (13), one has

$$\dot{\bar{z}}-\dot{u}_1=\dot{\bar{z}}-f_1(u_1,\boldsymbol{w}_1)-k(u_1-u_2)-d_1-I(t).\tag{14}$$

Because d_1 and d_2 are uncertain, the precise value of

$$\dot{\bar{z}}=\frac{\partial\bar{z}}{\partial u_2}(f_2(u_2,\boldsymbol{w}_2)+k(u_2-u_1)+d_2)+\frac{\partial\bar{z}}{\partial\boldsymbol{w}_2^{\rm T}}\boldsymbol{g}_2(u_2,\boldsymbol{w}_2)+k^{-1}(\dot{\widehat{d}}_2-a_1\dot{u}_{\rm d}-\ddot{u}_{\rm d})$$

cannot be obtained, where $\boldsymbol{w}_2=(w_2^1,w_2^2,\cdots,w_2^n)^{\rm T}$, $\frac{\partial\bar{z}}{\partial\boldsymbol{w}_2^{\rm T}}=(\frac{\partial\bar{z}}{\partial w_2^1},\frac{\partial\bar{z}}{\partial w_2^2},\cdots,\frac{\partial\bar{z}}{\partial w_2^n})$, and $\boldsymbol{g}_2(u_2,\boldsymbol{w}_2)=\dot{\boldsymbol{w}}_2$. Note that

$$\bar{\dot{z}}=\frac{\partial\bar{z}}{\partial u_2}(f_2(u_2,\boldsymbol{w}_2)+k(u_2-u_1)+\widehat{d}_2)+\frac{\partial\bar{z}}{\partial\boldsymbol{w}_2^{\rm T}}\boldsymbol{g}_2(u_2,\boldsymbol{w}_2)+k^{-1}(v_2-a_1\dot{u}_{\rm d}-\ddot{u}_{\rm d}).$$

Thus, Eq. (14) becomes

$$\dot{\bar{z}}-\dot{u}_1=\frac{\partial\bar{z}}{\partial u_2}(d_2-\widehat{d}_2)+\frac{1}{k}(\dot{\widehat{d}}_2-v_2)+\bar{\dot{z}}-f_1(u_1,\boldsymbol{w}_1)-k(u_1-u_2)-d_1-I(t).\tag{15}$$

When $I(t)=\bar{\dot{z}}-f_1(u_1,\boldsymbol{w}_1)-k(u_1-u_2)-\widehat{d}_1-I_0$, where I_0 is to be designed, one has

$$\dot{\bar{z}}-\dot{u}_1=\frac{\partial\bar{z}}{\partial u_2}(d_2-\widehat{d}_2)+\frac{1}{k}(\dot{\widehat{d}}_2-v_2)+(\widehat{d}_1-d_1)+I_0.$$

In this way, the system (1) (or equivalently the system (13)) changes to

$$\begin{cases}\dot{u}_2-\dot{u}_{\rm d}=-a_1(u_2-u_{\rm d})+k(\bar{z}-u_1)+d_2-\widehat{d}_2,\\ \dot{\bar{z}}-\dot{u}_1=\dfrac{\partial\bar{z}}{\partial u_2}(d_2-\widehat{d}_2)+\dfrac{1}{k}(\dot{\widehat{d}}_2-v_2)+(\widehat{d}_1-d_1)+I_0\end{cases}\tag{16}$$

with the following controller:

$$\begin{cases} I(t) = \bar{\dot{z}} - f_1(u_1, \boldsymbol{w}_1) - k(u_1 - u_2) - \widehat{d}_1 - I_0, \\ \bar{\dot{z}} = \dfrac{\partial \bar{z}}{\partial u_2}(f_2(u_2, \boldsymbol{w}_2) + k(u_2 - u_1) + \widehat{d}_2) + \dfrac{\partial \bar{z}}{\partial \boldsymbol{w}_2^{\mathrm{T}}}\boldsymbol{g}_2(u_2, \boldsymbol{w}_2) + k^{-1}(v_2 - a_1\dot{u}_{\mathrm{d}} - \ddot{u}_{\mathrm{d}}), \end{cases} \tag{17}$$

where $\bar{z}, v_2, \widehat{d}_1$, and $\widehat{d}_2$ are as mentioned above.

Furthermore, I_0 can be designed as follows:

$$I_0(t) = -\Big(\Big|\frac{\partial \bar{z}}{\partial u_2}\Big|\mu + \beta\Big)s_\alpha(\bar{z} - u_1), \tag{18}$$

where μ and β are positive numbers and satisfy $\mu > |d_2 - \widehat{d}_2|$ and $\beta > |\frac{1}{k}(\dot{\widehat{d}}_2 - v_2) + (\widehat{d}_1 - d_1)|$. This is reasonable according to Subsection 3.1. $s_\alpha(\cdot)$ denotes the saturation function, which is defined as

$$s_\alpha(x) = \begin{cases} \dfrac{x}{\alpha}, & \Big|\dfrac{x}{\alpha}\Big| \leqslant 1, \\ \mathrm{sign}\Big(\dfrac{x}{\alpha}\Big), & \Big|\dfrac{x}{\alpha}\Big| > 1, \end{cases}$$

where $\alpha > 0$.

The emphasis should be placed on the saturation function in the proposed controller. In the theory of sliding mode control, the saturation function can be replaced by the sign function, and a better result than that in Theorem 2 can be obtained. However, the sign function generates a chattering phenomenon caused by time delay, small disturbance and so on, when the trajectory is close to the objective trajectory. Although a small chattering phenomenon may not have great effects on the control effect, high-frequency chattering near the objective trajectory has a negative effect on the controller, and the controller will switch at a high frequency with a large amplitude. Thus, it is unreasonable to use the sign function in stimulating a neuron using the high-frequency potential with the large amplitude in practice.

Theorem 3 *For the system* (16) *under the controller defined by Eq.* (18), *that is, the system* (13) (*or the system* (1)) *under the controller defined by Eqs.* (17)–(18), *it holds that*

(I) *there exists a number* $T_4 \geqslant t_0$ *such that*

$$|\bar{z} - u_1| \leqslant \alpha \tag{19}$$

for $t \geqslant T_4$;

(II) *for* $a_1 > 0$ *and* $\forall \epsilon > 0$, *there exists a sufficiently large positive number* $T_5 > T_4$ *such that*

$$|u_2 - u_{\mathrm{d}}| < \epsilon + a_1^{-1}(|k|\alpha + k_2^{-1}\xi_2), \tag{20}$$

whenever $t > T_5$.

Proof (I) First, it is necessary to prove that there exists $T_4 \geqslant t_0$ such that

$$|\bar{z}(T_4) - u_1(T_4)| \leqslant \alpha. \tag{21}$$

Assume by contradiction that the statement of Eq. (21) is not true. Then, $\bar{z} - u_1 > \alpha$ or $\bar{z} - u_1 < -\alpha$ for all $t \geqslant t_0$. It is only necessary to prove the first case because the rest case can be proved with the same method. $\bar{z} - u_1 > \alpha$ holds for all $t \geqslant t_0$. Then, from the second expression of the system (16), one has

$$\dot{\bar{z}} - \dot{u}_1 = \frac{\partial \bar{z}}{\partial u_2}(d_2 - \widehat{d}_2) + \frac{1}{k}(\dot{\widehat{d}}_2 - v_2) + (\widehat{d}_1 - d_1) - \Big(\Big|\frac{\partial \bar{z}}{\partial u_2}\Big|\mu + \beta\Big) := \rho < 0, \tag{22}$$

and $\sup_{t>t_0}\rho(t)<0$. It follows that

$$\bar{z}-u_1=\bar{z}(t_0)-u_1(t_0)+\int_{t_0}^{t}\rho(\tau)\mathrm{d}\tau\leqslant\bar{z}(t_0)-u_1(t_0)+(t-t_0)\sup_{t>t_0}\rho(t)\to-\infty \tag{23}$$

as $t\to+\infty$. This is a contradiction for the hypothesis that $\bar{z}-u_1>\alpha$ holds for all $t>t_0$. That is to say, the inequality (21) is true.

Secondly, it is necessary to prove that Eq. (19) is true. Assume by contradiction that the statement of Eq. (19) is not true. Then, there exists $T_4'>T_4$ such that $\bar{z}(T_4')-u_1(T_4')>\alpha$ or $\bar{z}(T_4')-u_1(T_4')<-\alpha$. For the first case, there exists a T satisfying $T_4\leqslant T<T_4'$ such that $\bar{z}(T)-u_1(T)=\alpha$ and $\bar{z}(t)-u_1(t)>\alpha$ for $t\in(T,T_4')$. Thus, by the mean value theorem, there exists at least one $T'\in(T,T_4')$ such that $\dot{\bar{z}}(T')-\dot{u}_1(T')>0$. However, by Eq. (22), one has $\dot{\bar{z}}-\dot{u}_1<0$ for all $t\in(T,T_4')$. This is a contradiction. The second case can also be proved to be contradictory in a similar manner. Thus, Eq. (19) is true.

(II) From the proof of (i), one can conclude that

(i) if $|\bar{z}(t_0)-u_1(t_0)|>\alpha$, then $\bar{z}-u_1\leqslant|\bar{z}(t_0)-u_1(t_0)|$ for $t\in[t_0,T_4)$, which can be deduced with the same method as used for Eq. (23) and the result of (I);

(ii) if $|\bar{z}(t_0)-u_1(t_0)|\leqslant\alpha$, then Eq. (19) holds for $t\in[t_0,+\infty)$.

In this proof, we only consider the first case (the case (i)); the other case can be proved with the same method. According to the general solution formulae, the first expression of the system (16) can be rewritten as

$$\begin{aligned}u_2-u_\mathrm{d}=&\,\mathrm{e}^{-a_1(t-t_0)}(u_2(t_0)-u_\mathrm{d}(t_0))\\&+\int_{t_0}^{t}\mathrm{e}^{-a_1(t-\tau)}(k(\bar{z}(\tau)-u_1(\tau))+d_2(\tau)-\widehat{d}_2(\tau))\mathrm{d}\tau.\end{aligned}\tag{24}$$

Note that with Eq. (6), for $t>T_4$, one has

$$\begin{aligned}|u_2-u_\mathrm{d}|\leqslant&\mathrm{e}^{-a_1(t-t_0)}|(u_2(t_0)-u_\mathrm{d}(t_0))|+\int_{t_0}^{t}\mathrm{e}^{-a_1(t-\tau)}(|k||(\bar{z}(\tau)-u_1(\tau))|+|d_2(\tau)-\widehat{d}_2(\tau)|)\mathrm{d}\tau\\\leqslant&\mathrm{e}^{-a_1(t-t_0)}|(u_2(t_0)-u_\mathrm{d}(t_0))|+\int_{t_0}^{T_4}\mathrm{e}^{-a_1(t-\tau)}|k||(\bar{z}(\tau)-u_1(\tau))|\mathrm{d}\tau+\int_{T_4}^{t}\mathrm{e}^{-a_1(t-\tau)}\\&\cdot|k||(\bar{z}(\tau)-u_1(\tau))|\mathrm{d}\tau+\int_{t_0}^{t}\mathrm{e}^{-a_1(t-\tau)}(\mathrm{e}^{-k_2(\tau-t_0)}|(\widehat{d}_2(t_0)-d_2(t_0))|+k_2^{-1}\xi_2)\mathrm{d}\tau\\\leqslant&\mathrm{e}^{-a_1(t-t_0)}|(u_2(t_0)-u_\mathrm{d}(t_0))|+a_1^{-1}|k||\bar{z}(t_0)-u_1(t_0)|(\mathrm{e}^{-a_1(t-T_4)}-\mathrm{e}^{-a_1(t-t_0)})\\&+(a_1-k_2)^{-1}(\mathrm{e}^{-k_2(t-t_0)}-\mathrm{e}^{-a_1(t-t_0)})|(\widehat{d}_2(t_0)-d_2(t_0))|+a_1^{-1}(|k|\alpha+k_2^{-1}\xi_2).\end{aligned}$$

Thus, Eq. (20) is true, because $\mathrm{e}^{-a_1(t-t_0)}|(u_2(t_0)-u_\mathrm{d}(t_0))|+a_1^{-1}|k||\bar{z}(t_0)-u_1(t_0)|(\mathrm{e}^{-a_1(t-T_4)}-\mathrm{e}^{-a_1(t-t_0)})+(a_1-k_2)^{-1}(\mathrm{e}^{-k_2(t-t_0)}-\mathrm{e}^{-a_1(t-t_0)})|(\widehat{d}_2(t_0)-d_2(t_0))|\to0$ as $t\to+\infty$.

4 Simulation

As an application of the proposed control, the tracking control of the uncertain FHN model with one stimulus, described as

$$\begin{cases} \dot{u}_1 = c\Big(u_1 + w_1 - \dfrac{u_1^3}{3}\Big) + k(u_1 - u_2) + d_1 + I(t), \\ \dot{w}_1 = -\dfrac{1}{c}(u_1 - a + bw_1), \\ \dot{u}_2 = c\Big(u_2 + w_2 - \dfrac{u_2^3}{3}\Big) + k(u_2 - u_1) + d_2, \\ \dot{w}_2 = -\dfrac{1}{c}(u_2 - a + bw_2), \end{cases} \tag{25}$$

is studied, where $(a, b, c) = (0.7, 0.8, 3)$, the uncertain terms d_1 and d_2 are $d_1 = 0.1\sin(\frac{2\pi}{300}t)$ and $d_2 = -1.2 - 0.3\sin(\frac{2\pi}{30}t)$, and $k = 0.1$. To be more practical, the tracking signal is generated from the following modified ML model:

$$\begin{cases} \dot{V} = I - g(\mathrm{L})(V - E(\mathrm{L})) - g(\mathrm{K})w(V - E(\mathrm{K})) - g(\mathrm{Ca})m_\infty(V)(V - E(\mathrm{Ca})), \\ \dot{w} = \lambda(V)(w_\infty(V) - w), \\ \dot{u} = 0.005(0.2 + V), \end{cases} \tag{26}$$

where $I = -u$, $m_\infty(V) = \frac{1}{2}(1 + \tanh\frac{V - V_1}{V_2})$, $w_\infty(V) = \frac{1}{2}(1 + \tanh\frac{V - V_3}{V_4})$, $\lambda(V) = \frac{1}{3}\cosh\frac{V - V_3}{2V_4}$, and $(V_1, V_2, V_3, V_4, E(\mathrm{L}), E(\mathrm{Ca}), g(\mathrm{L}), g(\mathrm{K}), g(\mathrm{Ca})) = (-0.01, 0.15, 0.1, 0.05, -0.5, 1, 0.5, 2, 1.2)$. Two classical bursters for the desired action potential are tracked. The two bursters are called the "fold/Hopf" burster (see the blue solid lines in Fig. 2 with $E(\mathrm{K}) = -400$) and "fold/homoclinic" burster (see the blue solid lines in Fig. 3 with $E(\mathrm{K}) = -0.7$) according to the geometric bifurcation theory[5]. To classify the bursters, there are two important bifurcations involved, i.e., bifurcation from a quiescent state to repetitive spiking, and bifurcation from a spiking attractor to a quiescent state. A "fold/Hopf (homoclinic)" burster means that a fold bifurcation causes a neuron to change from a quiescent state to repetitive spiking, and a Hopf (homoclinic) bifurcation causes a neuron to change from a spiking attractor to a quiescent state. Usually, the two bifurcations can be analyzed by nullclines of fast subsystems and phase planes[26]. Our goal is to make $u_2 - V(:= u_\mathrm{d}) \to 0$ as $t \to +\infty$, as far as possible.

As shown in Eqs. (5) and (10), the observed values and the differentiated value only have connection with uncertainties d_1, d_2, and $\dot{\widehat{d}}_2$, and they have no connection with the state variables in the neuron model. Thus, we only give the case in the "fold/Hopf" burster. In the application of the control strategy proposed in Section 3, the parameter values are fixed, $(k_1, k_2, \gamma, \mu, \beta, \alpha, a_1) = (10, 10, 0.1, 2, 2, 0.5, 10)$. Figures 2 and 3 show that the "fold/Hopf" burster and "fold/homoclinic" burster generated by the ML model (26) (see the blue solid lines) have been tracked well and quickly by the second neuron in the FHN model (25) (see the red dotted lines). As shown in Figs. 4–6, the errors of estimation of the two observers and the differentiator are very small after a period of time. However, at the start, the error of estimation is relatively large. This is connected with the selection of initial values of the systems (2), (3), and (9).

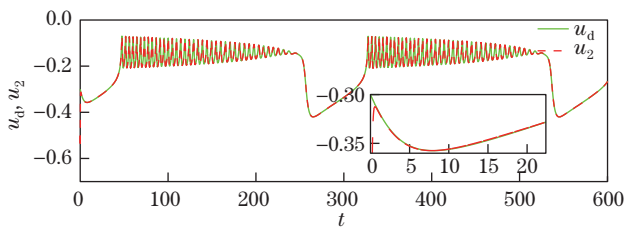

Fig. 2 Tracking the "fold/Hopf" burster (color online)

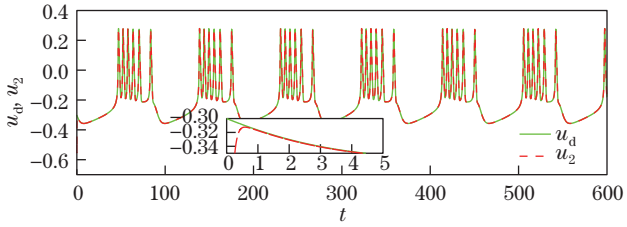

Fig. 3 Tracking the "fold/homoclinic" burster (color online)

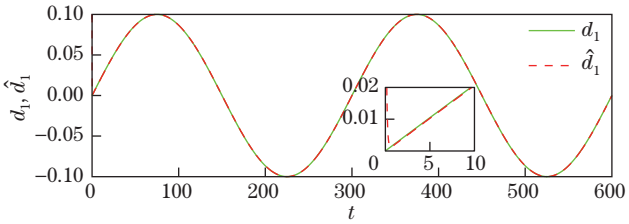

Fig. 4 The uncertainty d_1 and its observed value $\widehat{d_1}$ in the "fold/Hopf" burster (color online)

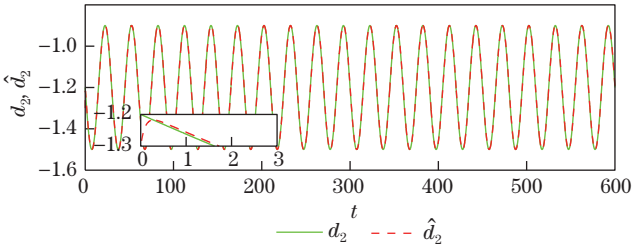

Fig. 5 The uncertainty d_2 and its observed value $\widehat{d_2}$ in the "fold/Hopf" burster (color online)

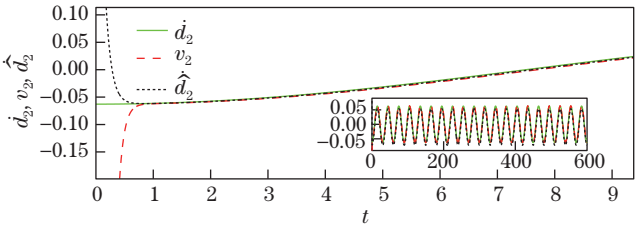

Fig. 6 $\dot{d}_2$, v_2 and $\dot{\widehat{d}}_2$ in the "fold/Hopf" burster (color online)

5 Conclusions

This study investigates the track control of the membrane potential of a neuron by stimulating an adjacent coupled neuron. Owing to the presence of uncertainties from model parameters and external disturbances, estimations of the uncertain terms are presented in terms of observers and a differentiator constructed using measured signals. The observers and differentiator are

primarily first-order low-pass filters, and the errors of their estimations depend on the characteristics of the uncertain terms only. In addition, a robust observer-based controller with a saturation function is presented for tracking the desired membrane potential, and it is robust against uncertainties. It is expected that the proposed controller might help in understanding the mechanism of neuronal control with a simple model, and more complex cases are left for future investigation.

Open Access This article is licensed under a Creative Commons Attribution 4.0 International License, which permits use, sharing, adaptation, distribution and reproduction in any medium or format, as long as you give appropriate credit to the original author(s) and the source, provide a link to the Creative Commons licence, and indicate if changes were made.

The images or other third party material in this article are included in the article's Creative Commons licence, unless indicated otherwise in a credit line to the material. If material is not included in the article's Creative Commons licence and your intended use is not permitted by statutory regulation or exceeds the permitted use, you will need to obtain permission directly from the copyright holder.

To view a copy of this licence, visit http://creativecommons.org/licenses/by/4.0/.

References

[1] HODGKIN, A. L., HUXLEY, A. F., and KATZ, B. Measurement of current-voltage relations in the membrane of the giant axon of Loligo. *Journal of Physiology*, **116**(4), 424–448 (1952)

[2] MORRIS, C. and LECAR, H. Voltage oscillations in the barnacle giant muscle fiber. *Biophysical Journal*, **35**(1), 193–213 (1981)

[3] FITZHUGH, R. Impulses and physiological states in theoretical models of nerve membrane. *Biophysical Journal*, **1**(6), 445–466 (1961)

[4] BERTRAM, R., BUTTE, M. J., KIEMEL, T., and SHERMAN, A. Topological and phenomenological classification of bursting oscillations. *Bulletin of Mathematical Biology*, **57**(3), 413–439 (1995)

[5] IZHIKEVICH, E. M. Neural excitability, spiking and bursting. *International Journal of Bifurcation and Chaos*, **10**(6), 1171–1266 (2000)

[6] CRUNELLI, V., KELLY, J. S., LERESCHE, N., and PIRCHIO, M. The ventral and dorsal lateral geniculate nucleus of the rat: intracellular recordings in vitro. *The Journal of Physiology*, **384**(1), 587–601 (1987)

[7] JOHNSON, S. W., SEUTIN, V., and NORTH, R. A. Burst firing in dopamine neurons induced by N-methyl-D-aspartate: role of electrogenic sodium pump. *Science*, **258**(5082), 665–667 (1992)

[8] RINZEL, J. Bursting oscillation in an excitable membrane model. *Ordinary and Partial Differential Equations*, Springer, New York, 304–316 (1985)

[9] DE VRIES, G. Multiple bifurcations in a polynomial model of bursting oscillations. *Journal of Nonlinear Science*, **8**(3), 281–316 (1998)

[10] RUSH, M. E. and RINZEL, J. Analysis of bursting in a thalamic neuron model. *Biological Cybernetics*, **71**(4), 281–291 (1994)

[11] ZEITlER, M., DAFFERTSHOFER, A., and GIELEN, C. C. Asymmetry in pulse-coupled oscillators with delay. *Physical Review E*, **79**(6), 065203 (2009)

[12] IZHIKEVICH, E. M. Subcritical elliptic bursting of Bautin type. *SIAM Journal on Applied Mathematics*, **60**(2), 503–535 (2000)

[13] REN, G., XU, Y., and WANG, C. Synchronization behavior of coupled neuron circuits composed of memristors. *Nonlinear Dynamics*, **88**(2), 893–901 (2017)

[14] FERRARI, F. A. S., VIANA, R. L., LOPES, S. R., and STOOP, R. Phase synchronization of coupled bursting neurons and the generalized Kuramoto model. *Neural Networks*, **66**, 107–118 (2015)

[15] IZHIKEVICH, E. M. Class 1 neural excitability, conventional synapses, weakly connected networks, and mathematical foundations of pulse-coupled models. *IEEE Transactions on Neural Networks*, **10**(3), 499–507 (1999)

[16] ERMENTROUT, B. Type I membranes, phase resetting curves, and synchrony. *Neural Computation*, **8**(5), 979–1001 (1996)

[17] CHAPIN, J. K., MOXON, K. A., MARKOWITZ, R. S., and NICOLELIS, M. A. L. Real-time control of a robot arm using simultaneously recorded neurons in the motor cortex. *Nature Neuroscience*, **2**(7), 664–670 (1999)

[18] HAO, Y. Y., ZHANG, Q. S., ZHANG, S. M., ZHAO, T., WANG, Y. W., CHEN, W. D., and ZHENG, X. X. Decoding grasp movement from monkey premotor cortex for real-time prosthetic hand control. *Chinese Science Bulletin*, **58**(20), 2512–2520 (2013)

[19] HAN, J. S. Acupuncture: neuropeptide release produced by electrical stimulation of different frequencies. *Trends in Neurosciences*, **26**(1), 17–22 (2003)

[20] XIE, Y., AIHARA, K., and KANG, Y. M. Change in types of neuronal excitability via bifurcation control. *Physical Review E*, **77**(2), 021917 (2008)

[21] HONG, K. S. Synchronization of coupled chaotic FitzHugh-Nagumo neurons via Lyapunov functions. *Mathematics and Computers in Simulation*, **82**(4), 590–603 (2011)

[22] CHEN, T., LIU, X., and LU, W. Pinning complex networks by a single controller. *IEEE Transactions on Circuits and Systems* I: *Regular Papers*, **54**(6), 1317–1326 (2007)

[23] SHI, X. and DAI, S. Intracellular solitary pulse calcium waves in frog sympathetic neurons. *Applied Mathematics and Mechanics* (*English Edition*), **26**(2), 150–159 (2005) https://doi.org/10.1007/BF02438236

[24] CHEN, W. H. and GUO, L. Control of nonlinear systems with unknown actuator nonlinearities. *IFAC Proceedings Volumes*, **37**(13), 1347–1352 (2004)

[25] ZHOU, Y. and WANG, Z. H. A robust optimal trajectory tracking control for systems with an input delay. *Journal of the Franklin Institute*, **353**(12), 2627–2649 (2016)

[26] SHI, M. and WANG, Z. H. Abundant bursting patterns of a fractional-order Morris-Lecar neuron model. *Communications in Nonlinear Science and Numerical Simulation*, **19**(6), 1956–1969 (2014)